Electromagnetic Scattering Controlling for a Rectangular Groove with High Impedance Surfaces Loading

Dongjiao Guo, Haiyan Chen, Peiheng Zhou,
Xingxing Huang, Jianliang Xie, and Longjiang Deng
National Engineering Research Center of Electromagnetic Radiation Control Materials
State Key Laboratory of Electronic Thin Film and Integrated Devices
University of Electronic Science and Technology of China, Chengdu 610054, China

Abstract— In this paper, a possible solution for controlling electromagnetic scattering from a rectangular groove is presented based on high impedance surfaces (HIS) loaded on the two sides of the considering groove. The HIS is realized by loading the H-shape frequency selective surfaces on a grounded dielectric layer, which is optimized according to the relationship between the scale parameters and its dispersion diagrams. The use of HIS resulting in a significant scattering suppression for the groove over a wide angular range for transverse magnetic (TM) polarization, and the maximum reduction of RCS can reach 17 dB compared with the original structure. Moreover, the monostatic radar cross section (RCS) reduction with the proposed method is superior to other methods such as loading resistive sheets.

1. INTRODUCTION

As a basic requirement of modern fighter aircraft, improving the stealth properties is becoming an inevitable trend. However, there are many scattering sources on the aircraft, such as angular diffraction, cavity scattering and specular reflection, which can cause strong electromagnetic (EM) scattering and contribute to the radar cross section (RCS) [1]. With the development of low observable technology, the main scattering sources mentioned above are effectively controlled, and the scattering resulting from surface defects such as groove is becoming a prominent part in total scattering, especially in some polarization and incident angles. Therefore controlling the scattering caused by groove is becoming an important issue in the stealth technology [2–4].

With the increase of study interest in controlling groove scattering, various measures are proposed. Among the most practical and commonly used technique is filling the groove with materials to form a smooth contoured exterior surface [5, 6]. However, in most cases filling the groove with materials cannot be fully achieved. For example, in military vehicles, discontinuities occur inevitably at the interface between two different materials where two dissimilar parts of the vehicle meet, such as the interface between a radome and the vehicle skin. For these considerations, there are also other methods that can reduce the groove radiation without affecting the total area. One of the methods is introducing a step of proper height between the medium and groove, and then filling the step with a material to make impedance-matching thus the radiation is reduced [7]. Besides, according to the transmission line theory, the scattering can also be controlled by loading the resistive sheets around the groove [8]. However, the ways proposed in [7, 8] only considered the scattering suppression in a single incident angle.

In this paper, a method of loading high impedance surfaces (HIS) to suppress groove scattering is proposed. Different from the method of impedance-matching to control groove scattering, the method proposed here is based on surface-wave bandgap properties of HIS [9] to hinder the propagation of surface waves. The HIS is optimized according to dispersion diagrams with different scale parameters. Then the scattering problem of HIS loading in different incident angles at TM polarization (the electric field vector is parallel to the plane of incidence) is analyzed, and the monostatic RCS is also calculated by method of moments (MOM), and is compared with the case of loading resistive sheets. Furthermore, the E-field intensity in the groove channel is also analyzed to validate this method.

2. DESIGN OF HIS

The building block of our design consists of a metallic array of sub-wavelength sized capacitive loaded strip (CLS) inclusions and a metal ground plane, separated by a dielectric spacer of relative permittivity ε_r, is shown in Fig. 1. The CLS inclusion has been chosen among others due to its well established and easily adjustable electromagnetic specifications [10, 11]. The size of a unit cell

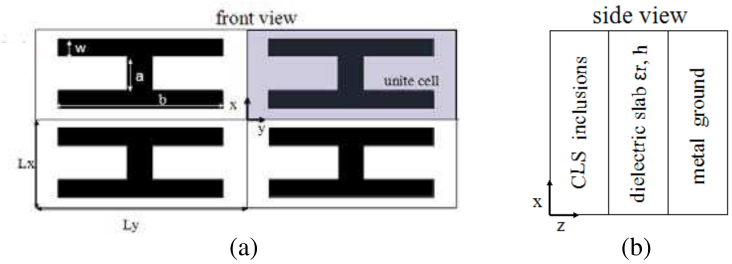

Figure 1: (a) Front view of the designed HIS. (b) Side view of the HIS.

is given by L_x and L_y. The dimension of a single CLS is determined by its vertical a and lateral b arm lengths, each being strips of width w.

An equivalent circuit model based on coupled microstrip line theory [12, 13] is used to design HIS. Through the optimization design, the structural parameters are taken as $L_x = 3.8$ mm, $L_y = 9$ mm, $w = 0.75$ mm, $a = 1.5$ mm, respectively, and the permittivity of the dielectric slab is taken as $\varepsilon_r = 3.9$.

The dispersion diagram of surface waves propagating along the periodic HIS structure is calculated by the eigenmode solution [14]. The simulation is based on a unit cell and assumes that the model extends to infinity in the x, y-plane through the application of periodic boundary conditions. Fig. 2 shows the behavior of the dispersion diagram as a function of the dimension parameter b. As shown in Fig. 2, the cut-off frequency of TM waves decreases with the increasing of parameter b. According to Figs. 2(a) and (b), we can see that the HIS support TM modes $kLx = 70°$ and $85°$ when $b = 5$ mm and 6 mm at the frequency of 10 GHz, the kLx can be defined in [9]. However, Figs. 2(c) and (d) show that there is no TM mode existing on the HIS structure in the cases of $b = 6.6$ mm and $b = 7$ mm in the frequency of 10 GHz, which meet the requirement of suppressing the propagation of TM surface waves. For the consideration of minimizing the size, we select the HIS of $b = 6.6$ mm to be loaded on the two sides of the groove.

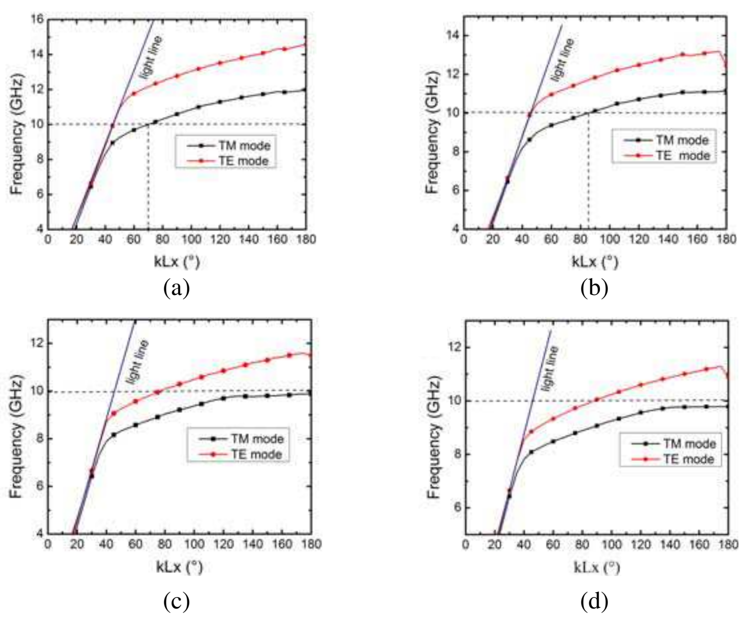

Figure 2: Dispersion diagrams of the HIS with different b. (a) $b = 5$ mm, (b) $b = 6$ mm, (c) $b = 6.6$ mm, (d) $b = 7$ mm.

3. RESULTS AND DISCUSSION

In this paper, the scattering properties of a rectangular groove in a finite perfect electric conductor (PEC) plate will be discussed, and its topology is shown in Fig. 3. Considered that strong EM radiation will be induced if the propagation direction of the incident waves is orthogonal to the edge of the plate, the groove is located at the diagonal position of the PEC plate.

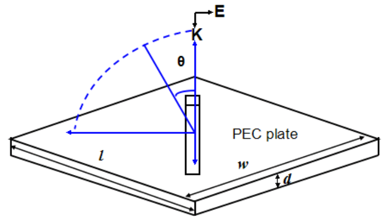

Figure 3: PEC plate with a rectangular groove. Parameters for the PEC plate are: $l = 130\,\text{mm}$, $w = 30\,\text{mm}$ and $d = 6\,\text{mm}$, parameters for the groove are: length $l' = 90\,\text{mm}$, width $w' = 5\,\text{mm}$ and depth $d' = 5\,\text{mm}$

Based on the MoM, the monostatic RCS of a rectangular groove in a finite PEC plate are computed, and the case of no groove PEC plate with similar size are also proposed for comparison, just as shown in Fig. 4. For small incident angles, the groove scattering is not apparent whether TE or TM polarizations, because the scattering is mainly caused by the specular reflection under this condition. For TE polarization, the existence of the groove has no obvious influence on the RCS with the increase of the incident angle, because the surface waves cannot exist on the PEC plate and the propagation through the groove is impossible. However, for TM polarization, the surface waves can emerge on the PEC plate and cause strong scattering when it go through the groove. The polarization-dependent phenomenon of the groove is consistent with the theory mentioned in [1]. Considering the polarization-dependent of the groove, only EM scattering properties of TM polarization is analyzed in the following discussion.

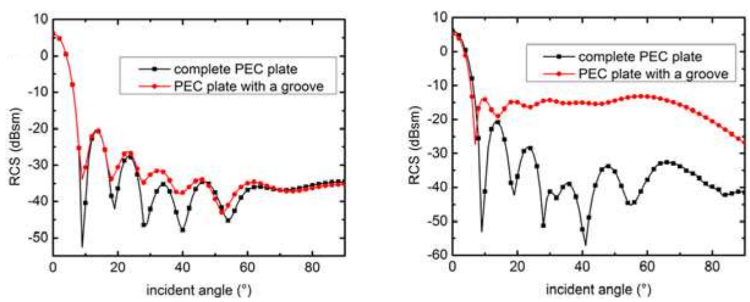

(a) (b)

Figure 4: Monostatic RCS of groove in PEC plate compared with a complete PEC plate for various incident angles. (a) TE-polarization, (b) TM-polarization.

Then the scattering properties of the finite metal groove with loading the designed HIS is discussed. The loading operation is performed in two stages. Firstly, two discontinuity steps between PEC plate and groove are introduced on the two sides of the groove, just as shown in Fig. 5(a). The structure dimensions of the introduced steps are $l = 90\,\text{mm}$, $a = 38\,\text{mm}$, $d = 1.5\,\text{mm}$. Nextly, the steps are filled with the designed HIS, just as shown in Fig. 5(b).

To identify the validity of HIS loading, it is necessary to compare the scattering results of the monostatic RCS with other conditions: the original structure and the case of filling the steps with resistive sheets proposed in [8]. As the Fig. 6 shows, in comparison with resistive sheets loading, the HIS loading can reduce the RCS over a wider angular range and the maximum reduction can reach 17 dB at the incident angle $\theta = 14°$.

Furthermore, in order to check whether the HIS loading reduces EM penetration through the groove, we calculate the E-field intensity at the middle plane inside the groove channel (Fig. 7(a)). Fig. 7(b) shows the E-field intensity inside the groove channel with and without HIS loading at the maximum RCS reduction angle of $\theta = 14°$, x and y represent the different positions in the calculated plane. As shown in Fig. 7, by HIS loading, the E-field intensity inside the groove channel is decreased nearly in all the positions, and the fields are significantly reduced at the front edge ($x = 2.5\,\text{mm}$) of the groove, thus leading to a reduction of the EM radiation induced by the groove. The variation in E-field intensity is consistent with the simulation results of monostatic RCS.

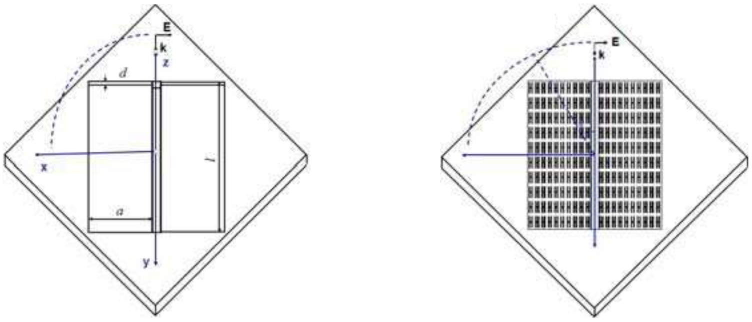

(a) (b)

Figure 5: The HIS loading operation. (a) The introduced steps. (b) Filling the steps with designed HIS.

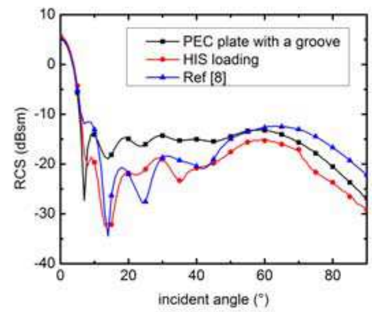

Figure 6: Scattering diagram from a rectangular groove with different loading.

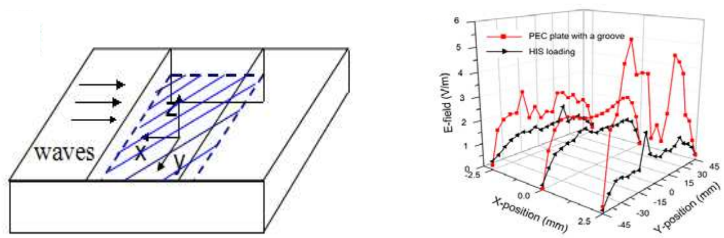

(a) (b)

Figure 7: E-field in the rectangular groove channel. (a) The calculated plane in the groove channel. (b) E-field in the calculated plane.

4. CONCLUSION

This paper presents a method of HIS loading to control EM scattering of grooves while maintaining the overall see-through size. The method is based on the surface-wave bandgap properties of HIS to suppress the surface waves penetrating through the groove. The HIS is optimized according to the dispersion diagrams with different structure parameters. The monostatic RCS with different loading are tested numerically using the MOM method. It is observed that a significant RCS reduction of up to 17 dB can be achieved in comparison to the case of the unloaded groove. Furthermore, compared the resistive sheets loading, the RCS reduction can be derived over a wider incident angular range. Finally, the E-field intensity in the groove channel is also analyzed and validate the proposed HIS loading for reducing the monostatic RCS of the groove target.

ACKNOWLEDGMENT

This research was partially supported by the National Natural Science Foundation of China (Grant No. 51301031) and the fundamental research funds (Project No. ZYGX2013J029).

REFERENCES

1. Knott, E. F., J. Shaeffer, and M. Tuley, *Radar Cross Section*, SciTech Publishing, 2004.
2. Richardson, D., *Stealth Warplanes*, Zenith Imprint, 2001.
3. Simpson, G. R., "Electromagnetic scattering from a gap in a magneto-dielectric coating on an infinite ground plane," No. AFIT/DS/ENG/02-03, Air Force Inst. of Tech. Wright-Patterson AFB (Ohio) School of Engineering, 2002.
4. Senior, T. B. A. and J. L. Volakis, "Scattering by gaps and cracks," *IEEE Transactions on Antennas and Propagation* Vol. 37, No. 6, 744–750, 1989.
5. Barkeshli, K. and J. L. Volakis, "Scattering from narrow rectangular filled grooves," *IEEE Transactions on Antennas and Propagation*, Vol. 39, No. 6, 804–810, 1991.
6. Choi, W.-H., et al., "Monostatic RCS reduction by gap-fill with Epoxy/MWCNT in groove pattern," *Journal of Electromagnetic Engineering And Science*, Vol. 12, No. 1, 101–106, 2012.

7. Kohin-Nitschelm, M., "Reduction of scatter from material discontinuities," U.S. Patent No. 5,570,092, Oct. 29, 1996.
8. Ramahi, O. M. and L. Li, "Analysis and reduction of electromagnetic field leakage through loaded apertures: A numerical study," *Electromagnetics*, Vol. 25, Nos. 7–8, 679–693, 2005.
9. Abhari, R. and G. V. Eleftheriades, "Metallo-dielectric electromagnetic bandgap structures for suppression and isolation of the parallel-plate noise in high-speed circuits," *IEEE Transactions on Microwave Theory and Techniques*, Vol. 51, No. 6, 1629–1639, 2003.
10. Ziolkowski, R. W., "Design, fabrication, and testing of double negative metamaterials," *IEEE Transactions on Antennas and Propagation*, Vol. 51, No. 7, 1516–1529, 2003.
11. Donzelli, G., et al., "Metamaterial made of paired planar conductors: Particle resonances, phenomena and properties," *Metamaterials*, Vol. 3, No. 1, 10–27, 2009.
12. Bahl, I. J., *Lumped Elements for RF and Microwave Circuits*, Artech House, 2003.
13. Hosseini, M. and M. Hakkak, "Characteristics estimation for Jerusalem cross-based artificial magnetic conductors," *IEEE Antennas and Wireless Propagation Letters*, Vol. 7, 58–61, 2008.
14. Remski, R., "Analysis of photonic bandgap surfaces using Ansoft HFSS," *Microwave J.*, Vol. 43, No. 9, 190–199, 2000.